NEOPLASIA
www.neoplasia.com

Volume 18 Number 5 May 2016 pp. 273–281 273

IL-6 Inhibition With MEDI5117 Decreases The Fraction of Head and Neck Cancer Stem Cells and Prevents Tumor Recurrence[1,2]

Kelsey A. Finkel[*], Kristy A. Warner[*], Samuel Kerk[*], Carol R. Bradford[†,#], Scott A. McLean[†,#], Mark E. Prince[†,#], Haihong Zhong[‡], Elaine M. Hurt[‡], Robert E. Hollingsworth[‡], Max S. Wicha[§,#], David A. Tice[‡] and Jacques E. Nör[*,†,¶,#]

[*]Department of Restorative Sciences, University of Michigan School of Dentistry, Ann Arbor, MI, USA; [†]Department of Otolaryngology, University of Michigan School of Medicine, Ann Arbor, MI, USA; [‡]MedImmune LLC, Gaithersburg, MD, USA; [§]Department of Internal Medicine, University of Michigan School of Medicine, Ann Arbor, MI, USA; [¶]Department of Biomedical Engineering, University of Michigan College of Engineering, Ann Arbor, MI, USA; [#]University of Michigan Comprehensive Cancer Center, Ann Arbor, MI, USA

Abstract

Head and neck squamous cell carcinomas (HNSCC) exhibit a small population of uniquely tumorigenic cancer stem cells (CSC) endowed with self-renewal and multipotency. We have recently shown that IL-6 enhances the survival and tumorigenic potential of head and neck cancer stem cells (*i.e.* $ALDH^{high}CD44^{high}$ cells). Here, we characterized the effect of therapeutic inhibition of IL-6 with a novel humanized anti-IL-6 antibody (MEDI5117) using three low-passage patient-derived xenograft (PDX) models of HNSCC. We observed that single agent MEDI5117 inhibited the growth of PDX-SCC-M1 tumors ($P < .05$). This PDX model was generated from a previously untreated HNSCC. In contrast, MEDI5117 was not effective at reducing overall tumor volume for PDX models representing resistant disease (PDX-SCC-M0, PDX-SCC-M11). Low dose MEDI5117 (3 mg/kg) consistently decreased the fraction of cancer stem cells in PDX models of HNSCC when compared to IgG-treated controls, as follows: PDX-SCC-M0 ($P < .001$), PDX-SCC-M1 ($P < .001$), PDX-SCC-M11 ($P = .04$). Interestingly, high dose MEDI5117 (30 mg/kg) decreased the CSC fraction in the PDX-SCC-M11 model ($P = .002$), but not in PDX-SCC-M0 and PDX-SCC-M1. MEDI5117 mediated a dose-dependent decrease in the number of orospheres generated by $ALDH^{high}CD44^{high}$ cells cultured in ultra-low attachment plates ($P < .05$), supporting an inhibitory effect on head and neck cancer stem cells. Notably, single agent MEDI5117 reduced the overall recurrence rate of PDX-SCC-M0, a PDX generated from the local recurrence of human HNSCC. Collectively, these data demonstrate that therapeutic inhibition of IL-6 with low-dose MEDI5117 decreases the fraction of cancer stem cells, and that adjuvant MEDI5117 inhibits recurrence in preclinical models of HNSCC.

Neoplasia (2016) 18, 273–281

Introduction

Head and neck squamous cell carcinoma (HNSCC) is a major health concern in the United States, with more than 40,000 new cases every year [1]. The standard of care for HNSCC includes intense platinum-based chemotherapy, complete surgical resection of the tumor (if possible), and radiotherapy [2]. Despite significant advances in treatment, the average 5-year survival for HNSCC patients has remained around 50% to 60% for the last 30 years [3]. Recognizing that the common causes of morbidity for patients with HNSCC is disseminated disease, recent research has focused on the understand-

Address all correspondence to: Jacques E. Nör DDS, PhD, Professor of Dentistry, Otolaryngology, Biomedical Engineering, University of Michigan, 1011 N. University Rm. 2309, Ann Arbor, MI, 48109–1078, United States. Tel.: +1 734 936 9300.
E-mail: jenor@umich.edu

[1] Financial support: This work was funded by a grant from MedImmune through the MedImmune-University of Michigan Agreement.
[2] Conflict of interest statement: David Tice, Haihong Zhong, Elaine Hurt, Robert Hollingsworth are employees of Medimmune, LLC. Max Wicha is an advisor for and has equity in OncoMed Pharmaceuticals. The remaining authors have no conflicts to declare.
Received 17 September 2015; Revised 7 March 2016; Accepted 14 March 2016

1476-5586
http://dx.doi.org/10.1016/j.neo.2016.03.004

ing of mechanisms regulating the tumorigenic process in search for better therapeutic targets. These studies led to the discovery of a small population of uniquely tumorigenic, multipotent cancer cells endowed with self-renewal, named cancer stem cells (CSC) [4,5]. These cells drive the tumorigenic process of HNSCC [6], and have recently become a conceptual target for therapy for patients with head and neck cancer. Considering the prominent role that cancer stem cells have on the dissemination of HNSCC [7], it is likely that patients with HNSCC will benefit from their targeted elimination.

Cancer stem cells proliferate slowly and are resistant to conventional therapies [8,9]. Indeed, we have recently observed that Cisplatin, the most frequently used chemotherapy for HNSCC, causes an increase in the CSC fraction in preclinical models [10]. Cisplatin treatment results in selective elimination of non-CSC as well as an increase in the self-renewal of CSCs, as demonstrated by enhanced expression of the major self-renewal regulator Bmi-1. These data led to the hypothesis that combination therapy with a tumor de-bulking strategy (*e.g.* chemoradiation) combined with an anti-cancer stem cell agent could provide a more durable response and enhance the survival of HNSCC patients [11].

Cancer stem cells are typically found in specialized niches, *i.e.* unique functional microenvironments that provide the cues required for survival and self-renewal of these cells [12,13]. We have observed that the majority of head and neck CSC are within close proximity of blood vessels, suggesting that these cells reside in perivascular niches [14]. Interestingly, endothelial cell-secreted factors, *e.g.* interleukin-6 (IL-6) and epidermal growth factor (EGF), activate key signaling pathways that protect CSC from anoikis and enhance their invasive potential [15–17]. Further, IL-6 is more highly expressed in the vascular endothelial cells of head and neck tumors than in the tumor cells themselves [17]. IL-6 activates the STAT signaling pathway via the JAK kinase. The activation of JAK leads to downstream phosphorylation of the STAT3, which is translocated to the nucleus to regulate genes critical in controlling cell proliferation, differentiation, and survival signals [18]. We have recently shown that endothelial cell-secreted IL-6 enhances the tumorigenic potential and self-renewal of head and neck CSC [17]. In addition, IL-6 potentiates the inductive effect of Cisplatin on the self-renewal of CSC, resulting in accumulation of these cells [10]. From a clinical perspective, a strong correlation between high serum IL-6 levels with poor survival of head and neck cancer patients has been reported [19].

Collectively, these studies provide strong rationale for the development of anti-IL-6 therapies for treatment of patients with HNSCC. Here, we evaluated the effect of MEDI5117, a novel humanized monoclonal antibody with high affinity for IL-6 [20], on the CSC fraction and recurrence of patient-derived xenograft (PDX) tumor models of HNSCC. MEDI5117 was generated by variable domain engineering (to enhance its affinity for IL-6), in combination with the use of Fc (fragment crystallizable) engineering that aimed at enhancing the half-life of the antibody and therefore allowing for lower frequency of administration [20]. Indeed, MEDI5117 might be considered an example of a "next-generation" antibody that could be well suited for long-term use as a CSC-targeting strategy since it is not associated with significant systemic toxicities.

Materials and Methods

Patient-Derived Xenograft (PDX) Tumor Models of HNSCC

Patient-derived xenograft (PDX) tumor models (PDX-SCC-M series) were generated from HNSCC tumors that were surgically resected between August/2012 and May/2013 at the University of Michigan (Supplementary Figure 1). The collection and handling of these specimens was performed under signed, informed consent and approval from appropriate institutional review boards. Tumors were minced into small pieces (4 mm × 4 mm) and washed 2–3 times in primary tumor medium consisting of high glucose Dulbecco's Modified Eagle's Medium (DMEM; Invitrogen; Carlsbad, CA, USA), supplemented with 1% L-glutamine (Invitrogen), 10% Fetal Bovine Serum (Invitrogen), 20 ng/ml rhEGF (Sigma-Aldrich; St. Louis, MO, USA), 400 ng/ml hydrocortisone (Sigma-Aldrich), 5 μg/ml insulin (Sigma-Aldrich), 50 mg/ml Nystatin (Sigma-Aldrich), antibiotic-antimycotic (AAA; Sigma-Aldrich) and amphotericin-B (Sigma-Aldrich). After washing, tumor fragments were transplanted into the subcutaneous space of the dorsal region of severe combined immunodeficient mice (CB-17 SCID; Charles River; Wilmington, MA, USA). Tumors were surgically retrieved when they reached 700 to 1000 mm^3, and passed serially into new mice. Notably, all experiments included here were performed in PDX tumors at *in vivo* passage 6 or lower. Tumor, liver, and lung tissues were retrieved and fixed overnight in 10% phosphate-buffered formalin (Fisher; Waltham, MA, USA) at 4°C and processed for immunohistochemistry.

Short-Tandem Repeat (STR) Profiling

To verify the identity of the PDX models over several *in vivo* passages, genomic DNA from the patient's tumor or Passage 0 xenograft (reference) and subsequent passages of xenograft tumors was purified using the Wizard Genomic DNA Purification Kit (Promega; Madison, WI, USA). DNA genotyping by short tandem repeat (STR) profiling was performed and analyzed independently by Genetica LabCorp (Burlington, NC, USA).

TruSeq Amplicon-Cancer Panel (TSACP) Assay

The TruSeq Amplicon-Cancer Panel (TSACP) assay (Illumina; San Diego, CA, USA) was performed to detect specific mutations in a panel of 48 cancer-related genes in our PDX models of HNSCC. Data were analyzed by the MiSeq desktop sequencer (Illumina), as recommended by the manufacturer.

MEDI5117 Treatment

Mice harboring PDX tumors (approximately 200 mm^3) were treated with 3 or 30 mg/kg MEDI5117 (MedImmune; Gaithersburg, MD, USA) injected intraperitoneally, two times per week, for 3 to 7 weeks to evaluate the effect of this antibody on tumor growth and cancer stem cell fraction. Alternatively, tumors were allowed to grow to approximately 700 mm^3 and then surgically removed to evaluate the effect of MEDI5117 on tumor recurrence.

Immunofluorescence

For CSC staining, tissues were exposed to 3% hydrogen peroxide (Fisher), and incubated overnight at 4°C with a rabbit anti-ALDH1 antibody (1:50; Abcam; Cambridge, MA, USA). ALDH1 signal was detected with Alexafluor 488 secondary antibody (1:200; Invitrogen). Then, tissues were incubated with a mouse anti-CD44 antibody (Thermo Scientific; Wayne, MI, USA). CD44 signal was detected with Alexafluor 594 secondary antibody (1:200; Invitrogen). Slides were mounted with ProLong Gold Anti-fade Reagent with DAPI (Invitrogen) before imaging.

Head and Neck Cancer Stem Cell Sorting

Primary human HNSCC specimens were cut and minced with a sterile scalpel until they could pass through a 25 ml pipette. They were dissociated using the GentleMACS kit (Miltenyi; Bergisch

Gladbach, Germany) and GentleMACS dissociator (Miltenyi). Cells were filtered through a 40-μm nylon sieve (BD Biosciences, San Jose, CA, USA), washed with DMEM, and centrifuged at 800 RPM, 4°C for 5 minutes. Red blood cells were lysed for 1 minute using 5 ml AKC lysing buffer (Invitrogen) and centrifuged at 800 RPM, 4°C for 5 minutes. Resulting single cell suspensions were washed, counted, and resuspended at 1×10^6 cells/ml in PBS. The Aldefluor kit (Stem Cell Technologies; Vancouver, BC, Canada) was used to identify cells with high ALDH activity. Briefly, cells were suspended in activated BAAA-DA substrate or in a specific ALDH inhibitor (DEAB, Stem Cell Technologies) for 45 minutes at 37°C. Cells were then exposed to anti-CD44 (clone G44-26, BD Biosciences; San Jose, CA, USA) and HLA-ABC to select for human cells. Finally, 7-Aminoactinomycin (7-AAD; BD Biosciences) was used to eliminate non-viable cells. Cancer stem cells were identified as the subpopulation of cells expressing high levels of ALDH and CD44, as we have shown previously [14,17].

Enzyme-Linked Immunosorbent Assay (ELISA)

Nunc Maxisorb plates (eBioscience; San Diego, CA, USA) were coated with 100 μl of 1 μg/ml MEDI5117 and incubated overnight at 4°C. After 4 washes, 100 μl of standard (eBioscience) or tumor lysate was added to the plates. We sealed the plates and incubated them for 2 hours at room temperature. Washed cells were then exposed to 100 μl of detection antibody (Cell Sciences; Canton, MA, USA) and incubated for 1 additional hour at room temperature. Following this incubation, plates were again washed. We added 100 μl Avidin-HRP (eBioscience) to each plate and incubated at room temperature for 30 minutes. After a final wash, 100 μl of TMB substrate solution (eBioscience) was added to the wells. After 15 minutes, 50 μl of stop solution was added to the plates. Absorbance was measured immediately on a microplate reader at 450 nm with a subtraction of 562 nm (Genios Tecan; Salzburg, Austria). Triplicate wells per tumor lysate were evaluated.

Sulforhodamine-B (SRB) Assay

For these studies, we plated 2×10^3 HNSCC cells per well (UM-SCC-11B or UM-SCC-22B, kindly provided by Dr. T. Carey) and exposed them to 0.01 to 100 μg/ml MEDI5117 or 100 μg/ml control IgG (R347). After 24 to 72 hours, cells were fixed with 50% trichloroacetic acid and stained with 0.4% sulforhodamine-B solution (SRB; Sigma Aldrich). Unbound SRB dye was removed by washing with 1% acetic acid. Plates were air-dried and bound SRB was resolubilized in 10 mM unbuffered Trizma base. Absorbance was analyzed on a microplate reader at 560 nm (Genios Tecan). Test results were normalized against initial plating density and IgG controls. Quadruplicate wells per condition were evaluated and are representative of at least two independent experiments.

Orosphere Assay

Non-adherent spheroids of head and neck cancer stem-like cells (named orospheres) were generated from FACS-sorted UM-SCC-22B cells (1×10^3 cells/well) and cultured in triplicate wells in 24-well ultra-low attachment plates (Corning, Corning, NY, USA), as we have shown previously [21]. Briefly, cells were cultured in DMEM/F12 (Invitrogen) supplemented with 1% N2 (Invitrogen), 10 ng/ml EGF (Sigma-Aldrich), and 10 ng/ml basic Fibroblast Growth Factor (bFGF; EMD Millipore, Temecula, CA, USA). After 3 days, orospheres (defined as spheres of ≥25 cells) were visualized and quantified under light microscopy, then treated with 0.01 to 100 μg/ml MEDI5117 (MedImmune) or 100 μg/ml IgG control (MedImmune). After 3 to 5 additional days, orospheres were again visualized and quantified under light microscopy. Alternatively, cells were treated with MEDI5117 or IgG control at the time of plating. After 3 to 7 days, orospheres were visualized and quantified under light microscopy.

Statistical Analyses

Data were analyzed by one-way analysis of variance (ANOVA) followed by appropriate post-hoc tests. Kaplan Meier analyses were performed to determine the effect of treatment on time to tumor recurrence. Statistical significance was determined at $P < .05$. These analyses were performed using the SigmaStat 2.0 software (SPSS; Chicago, IL, USA).

Results

Characterization of the PDX Models of Head and Neck Squamous Cell Carcinoma

To generate patient-derived xenograft (PDX) models of HNSCC, we implanted small fragments of the primary tumor directly in the subcutaneous space of immunodeficient mice. The primary tumors used to generate the PDX models represent diverse clinical characteristics typically observed in patients with HNSCC. The PDX-SCC-M1 model was generated from the primary tumor of a patient that was previously untreated. The PDX-SCC-M0 model was generated from the local recurrence of a patient that had incomplete resection of the primary tumor without radiation or chemotherapy. Lastly, the PDX-SCC-M11 model represents a local recurrence of a primary tumor in the sinonasal cavity of a patient who previously underwent treatment with surgery, radiation, and chemotherapy with TPF (Docetaxel, Carboplatin, 5-Fluorouracil) (Supplementary Figure 1). The rationale for selecting these 3 models is based on our intent to rigorously test the effect of MEDI5117 across a spectrum of different possible clinical manifestations of HNSCC. We performed serial passaging of the PDX tumors for up to 8 *in vivo* passages (Figure 1*A*), but only used PDX tumors up to passage 6 for the testing of MEDI5117. The overall micromorphology of the PDX tumor models across numerous passages was consistent with the original human tumors (Figure 1*B*). As we have shown with salivary gland cancer [22], overall trends of faster tumor growth (Figure 1*A*) and enhanced tumor take (data not shown) were observed with increased *in vivo* passaging of the PDX models. To determine if the PDX models are reflective of their primary source, and to evaluate potential genetic drifts over time, short tandem repeat (STR) profiling was performed (Supplementary Figure 2A). Based on the analysis of 15 autosomal loci and the gender identity locus Amelogenin, the STR profiles for PDX-SCC-M0 and PDX-SCC-M11 showed 100% match against the respective reference samples. We observed minimal allelic loss (94.3% match) in the PDX-SCC-M1 model. This phenomenon has been reported as the result of a mouse DNA increase relative to the human DNA content, which typically happens in xenograft tumors [23]. Notably, all three patient samples used for generation of the PDX models characterized here were negative for HPV16 (data not shown), which typically correlates with head and neck tumors that are resistant to therapy [24].

To begin to characterize the mutational landscape of our PDX models of HNSCC, we performed targeted sequencing using the MiSeq platform. We used the Cancer Panel from Illumina and therefore the genes that were sequenced constitute a panel of 48 of the

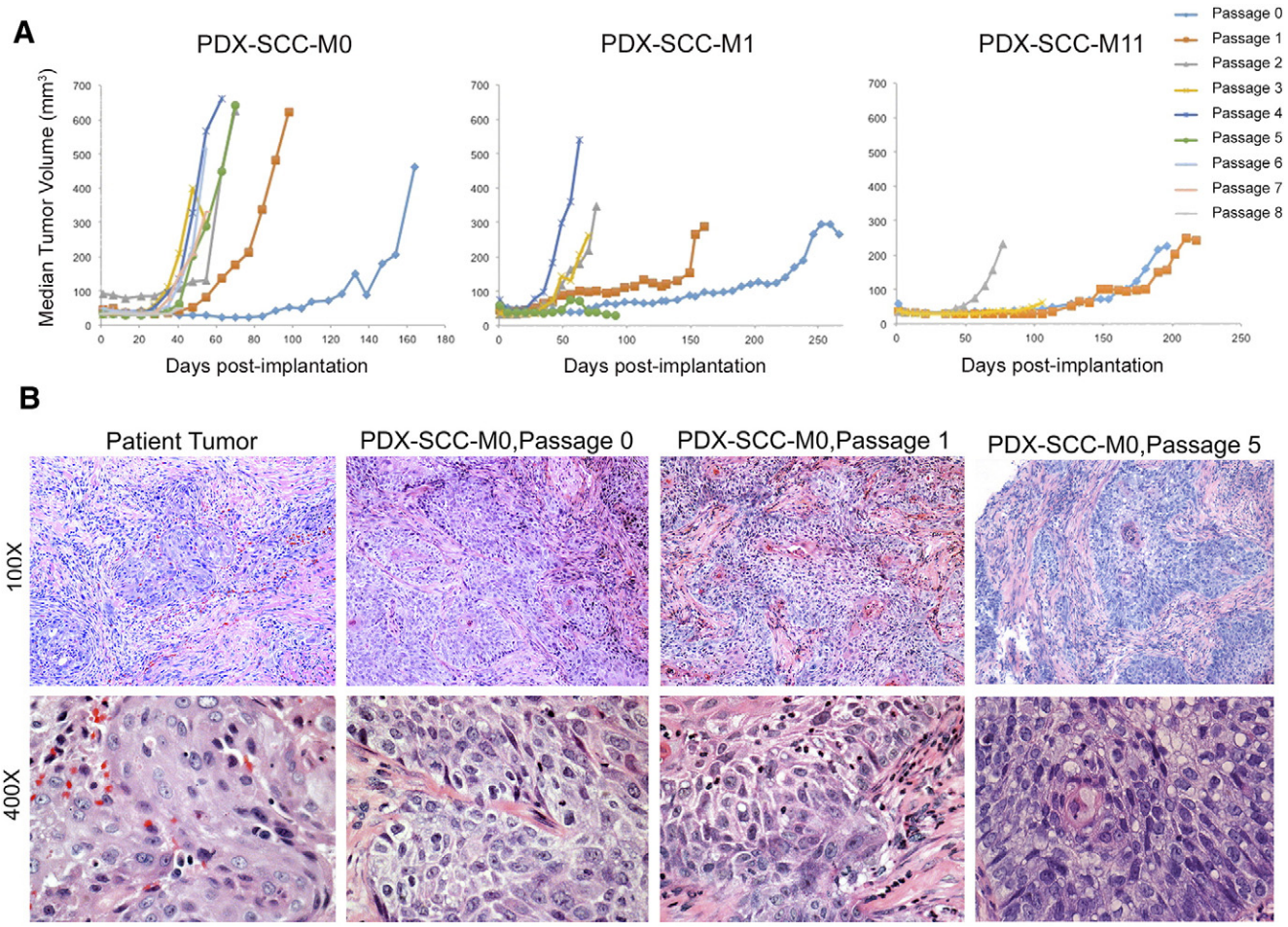

Figure 1. Characterization of the PDX models of head and neck squamous cell carcinoma. (A) Graphs depicting tumor growth over time. Lines represent the median tumor volumes within each passage of the PDX models of HNSCC used here. (B) H&E staining of the original human tumor and correspondent PDX-SCC-M0 model at passage 0, 1 and 5. Please note that the overall micromorphology of the PDX tumor closely resembles the morphology of the human tumor used to generate the PDX model.

most frequently mutated genes in cancer, including in HNSCC [25]. PDX-SCC-M0 exhibited a non-synonymous mutation of *AKT1* that was carried through from Passage 0 to Passage 5 xenografts (Supplementary Figure 2B). Three mutations (*TP53, FGFR3, GNAS*) were observed in PDX-SCC-M1 tumors. Notably, all of these mutations are in genes that regulate critical cell survival and differentiation pathways. For example, *TP53* is a key regulator of cell apoptosis and it is the most frequently mutated gene in HNSCC [25].

Low Dose MEDI5117 Decreases the Fraction of Cancer Stem Cells in PDX Models of Head and Neck Squamous Cell Carcinoma

We have previously shown that ALDH^{high}CD44^{high} cells sorted from HNSCC are multipotent, exhibit self-renewal, and are highly tumorigenic, characterizing this sub-population as cancer stem cells [14]. We used low-passage (up to passage 6) PDX models to evaluate if treatment with MEDI5117 affects tumor growth and the fraction of CSC. The PDX tumors consistently showed high fractions of CD44-positive cells, and few ALDH1-positive cells (Figure 2). Treatment with single agent MEDI5117 caused a significant inhibition of tumor growth in the PDX-SCC-M1 model, but not in the PDX-SCC-M0 or PDX-SCC-M11 models (Figure 3*A*; Supplementary Figure 3). As expected, MEDI5117 reduced the levels of circulating free IL-6 (Supplementary Figure 4). MEDI5117 at a dose of 3 mg/kg consistently caused a decrease in the fraction of cancer stem cells (ALDH^{high}CD44^{high}) in the PDX-SCC-M11 model (P = .04), PDX-SCC-M1 model (P < .001) and PDX-SCC-M0 (P < .001) (Figure 3*C*). Surprisingly, at the higher dose of 30 mg/kg, MEDI5117 caused a decrease in cancer stem cell fraction in the PDX-SCC-M11 model (P = .002), but not in the PDX-SCC-M0 or PDX-SCC-M1 models (P > .05) (Figure 3*C*). Both regimens for MEDI5117 were very well tolerated by the mice, as demonstrated by the absence of noticeable weight loss (compared to IgG controls) for the duration of the experiments, *i.e.* up to 126 days (Figure 3*B*).

Effects of MEDI5117 on Sorted and Unsorted HNSCC Cells

To evaluate the effect of MEDI5117 on the proliferation/survival of HNSCC cells, we exposed two established cell lines (UM-SCC-11B, UM-SCC-22B) to increasing concentrations of the antibody and performed the SRB assay. We observed that MEDI5117 did not show a demonstrable impact on unsorted HNSCC cell density (Figure 4*A*). We repeated this assay with low passage primary cells that outgrew from the PDX tumors models used

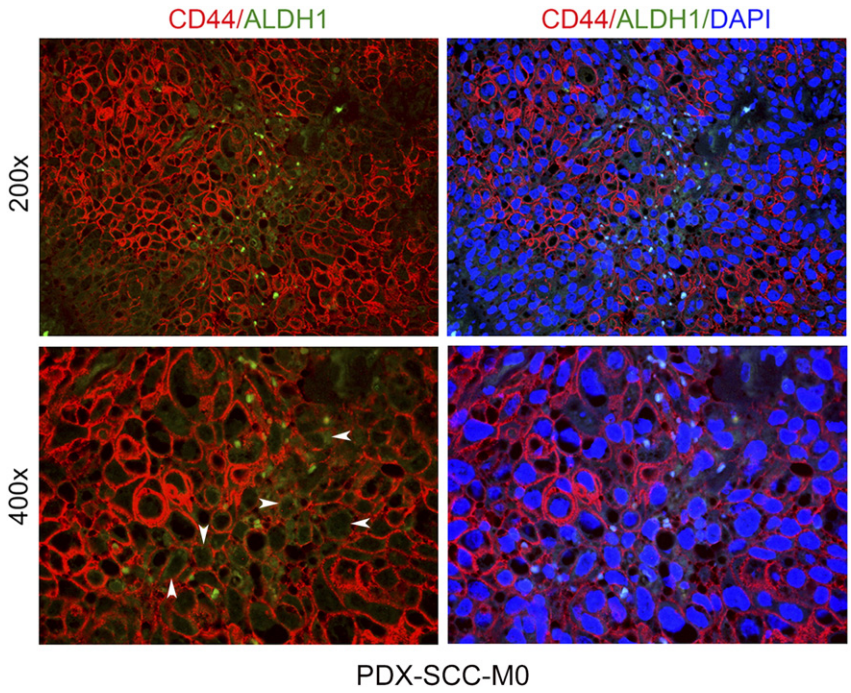

Figure 2. Expression of ALDH1 and CD44 in a PDX model of HNSCC. Immunofluorescence staining of ALDH1 (green) and CD44 (red) in histological sections of the PDX-SCC-M0 model at 200 × and 400 × magnifications. White arrowheads point to $ALDH^{high}CD44^{high}$ cells. Please note the cytoplasmic localization of ALDH1 and the cell membrane localization of CD44. DAPI (blue) was used to identify cell nuclei.

here, and again we did not see any impact on the density of unsorted cells (data not shown).

To evaluate the effect of MEDI5117 on CSC, we used the orosphere assay with cells sorted for ALDH and CD44 grown in ultra-low attachment plates [21]. We observed a significant decrease in the number of orospheres when MEDI5117 was added to the medium at the time of cell plating (Figure 4*B*). To challenge these results, we repeated this experiment but now we allow the orospheres to form for 3 days and then we added MEDI5117. We observed that MEDI5117 was able to disrupt the orospheres causing a significant decrease in their number (Figure 4*B*). Notably, control non-CSC $ALDH^{low}CD44^{low}$ cells formed very few orospheres under low attachment conditions, and no effect for MEDI5117 was observed in these cells (Figure 4*B*). Collectively, this set of experiments demonstrated that MEDI5117 has a more prominent effect on the cancer stem cells, as compared to broad effects in the bulk cells.

Next, we examined the effect of MEDI5117 on the activation of the STAT3 pathway in HNSCC cells (Figure 4*C*). UM-SCC-11B and UM-SCC-22B were starved overnight before being exposed to recombinant human IL-6 (rhIL-6) in presence of MEDI5117 or IgG. As expected, exposure to rhIL-6 resulted in STAT3 phosphorylation. MEDI5117 mediated a potent decrease in STAT3 phosphorylation in both cell lines *in vitro*. The same phenomenon was observed *in vivo*, in PDX-SCC-M11 tumors from mice treated with MEDI5117 (Figure 4*D*). We also observed some decrease in expression of the receptor IL-6R in mice treated with MEDI5117 (Figure 4*D*).

MEDI5117 Prevents Tumor Recurrence When Used in the Adjuvant Setting

Considering the emerging evidence demonstrating a prominent role for cancer stem cells in HNSCC tumor cell invasion [16,26] and dissemination [7], we designed pre-clinical trials intended to verify the effects of MEDI5117 on HNSCC recurrence (Figure 5). PDX-SCC-M0 tumors were allowed to grow up to a mean volume of 700 mm^3 before being surgically resected (Figure 5*A*). MEDI5117 was administered either in a *neoadjuvant* setting (treatment started 2 days prior to surgery) or *adjuvant* setting (treatment started 1 day after surgery). Mice from both groups were treated equally with MEDI5117 thereafter. The IgG control group received its first dose 1 day following surgical resection of the tumors, mimicking the adjuvant setting. Treatment with MEDI5117 continued twice weekly for seven weeks following tumor resection, and mice were monitored two times per week for tumor recurrence for up to 100 days. A Kaplan-Meier analysis was performed using the presence of a palpable tumor (Supplementary Figure 5) as criteria for tumor recurrence. We observed that MEDI5117 in the adjuvant setting did not allow any tumor recurrence (0 out of 9 mice with palpable tumors) for at least 100 days after surgical removal of the original tumor (P = .0068) (Figure 5*C*). In contrast, tumor recurrence was observed when MEDI5117 was used in the neoadjuvant setting (4 out of 10) and when IgG control was used (P = .2485) (6 out of 10) (Figure 5*C*). Notably, when all MEDI5117-treated tumors were grouped together (19 tumors), we observed a significant (P = .0172) inhibition of tumor recurrence when compared to all IgG control tumors (Figure 5*C*).

Discussion

Advanced primary HNSCC initially responds well to chemoradiation. However, a frequent problem with these patients is local recurrence and/or distant metastases. Emerging evidence supports a key role for CSC in the dissemination of HNSCC [7,16,26]. Here, we showed that low dose monoclonal anti-IL-6 antibody reduces the

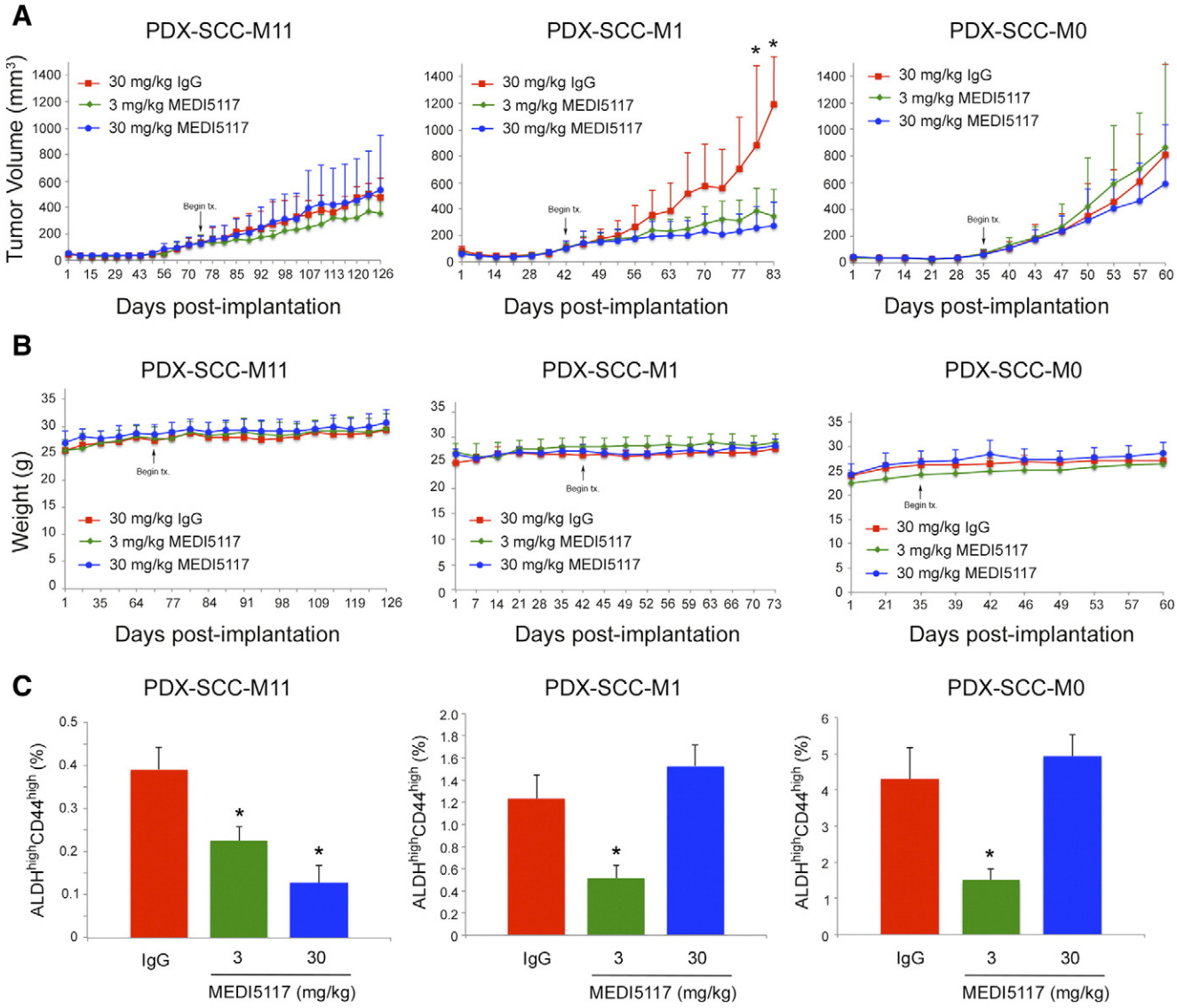

Figure 3. Low dose MEDI5117 decreases the fraction of cancer stem cells in PDX models of HNSCC. (A) Graphs depicting mean tumor growth over time in mice treated with 3 or 30 mg/kg MEDI5117, as compared to treatment with IgG control. Arrows denote the timing for the beginning of treatment with MEDI5117 or IgG control. (B) Graphs depicting mean mouse weight according to treatment conditions over time. (C) Graphs depicting the percentage of $ALDH^{high}CD44^{high}$ cells, as determined by flow cytometry from 5 tumors (PDX-SCC-M1 and PDX-SCC-M11) or 6 tumors (PDX-SCC-M0). Asterisks depict $P < .05$.

CSC fraction in PDX models of HNSCC and prevents recurrence when used in the adjuvant setting after surgical removal of the primary tumor. These results suggest that patients with HNSCC might benefit from therapeutic inhibition of IL-6 with a monoclonal antibody.

We developed and characterized 3 new PDX models of HNSCC for the work presented here. These models were generated from patients with advanced HNSCC (Stage III or IV) and represent three distinct clinical scenarios that are relatively common in this patient population. We believe that these PDX models are representative of patients that typically do not respond well to treatment, and are therefore useful for rigorous testing of new therapies. Furthermore, we have treated only low passage (*i.e.* less than 6 *in vivo* passages) PDX tumors in an attempt to more accurately recapitulate the disease encountered in a clinical setting. We observed that MEDI5117 inhibited the growth of the PDX-SCC-M1 model that was generated from a previously untreated patient with advanced HNSCC (Stage III). In contrast, the PDX-SCC-M0 and PDX-SCC-M11 models that represent previously treated, recurrent tumors were not responsive to treatment with MEDI5117. These results suggest that MEDI5117 has modest effects on previously treated tumors, and would likely have to be combined with conventional therapies in these settings.

The analysis of the effect of MEDI5117 in CSC revealed interesting results. While MEDI5117 had no measurable effect in unsorted HNSCC cells, we observed consistent inhibitory activity of MEDI5117 in sorted CSC using the orosphere assay. These data suggest that the effect of MEDI5117 might be primarily observed in CSC. Interestingly, we have previously shown that head and neck CSC ($ALDH^{high}CD44^{high}$) express significantly higher levels of IL-6R than non-CSCs ($ALDH^{low}CD44^{low}$) [17], which might explain, at least in part, the selective effect of MEDI5117 in the CSC population.

We observed that single agent MEDI5117 was sufficient to prevent tumor growth in the PDX model of previously untreated disease

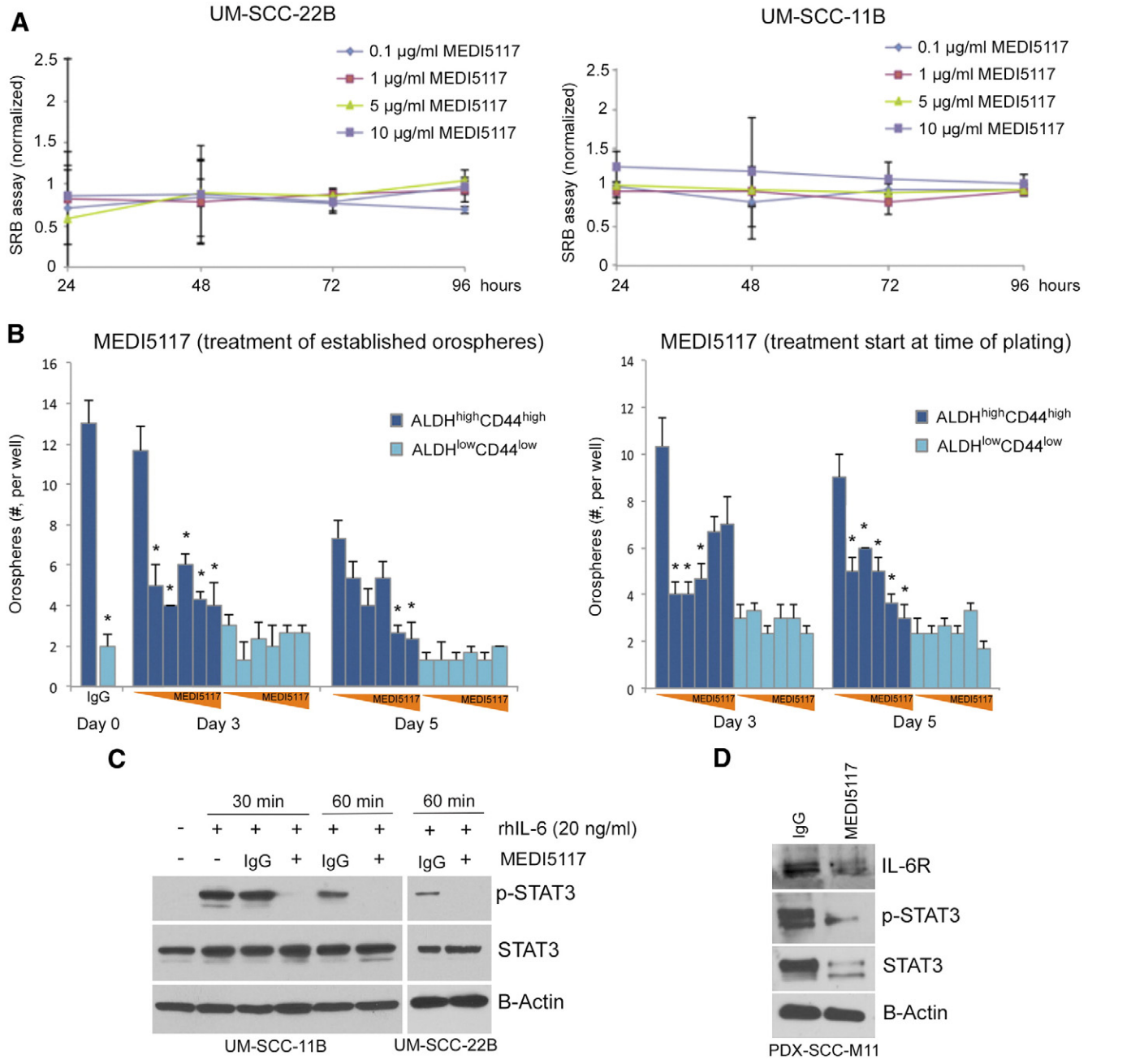

Figure 4. Effects of MEDI5117 on overall survival, number of orospheres, and STAT3 signaling in HNSCC cells. (A) Graphs depicting the effect of 0.1-10 μg/ml MEDI5117 on bulk cell survival of unsorted HNSCC cells (UM-SCC-11B, UM-SCC-22B), as determined by SRB assay. Data were normalized against corresponding IgG controls. (B) Graphs depicting the effect of MEDI5117 on HNSCC cells (UM-SCC-22B) sorted for ALDH and CD44. Cells were treated with increasing concentrations of MEDI5117 (0.01–10 μg/ml) or 10 μg/ml IgG control either after formation of orospheres (left panel) or at the time of plating (right panel) in 24-well ultra-low attachment plates (n = 3 wells/condition). Significance was determined by one-way ANOVA to the control within each day. Asterisks depict $P < .05$. (C) Western blots depicting the effect of treatment with MEDI5117 on phospho- and total STAT3 in UM-SCC-11B and UM-SCC-22B cells. Cells were treated with 0 or 20 ng/ml rhIL-6 in presence of 0 or 10 μg/ml MEDI5117 for 24 hours (D) Western blot depicting the *in vivo* effect of MEDI5117 on IL-6R, pSTAT3, and total STAT3 expression in PDX-SCC-M11 tumors from mice treated either with 3 mg/kg MEDI5117 or IgG control.

(PDX-SCC-M1). In contrast, MEDI5117 was not able to slow down tumor growth in the two tumor-resistant PDX models studied here (PDX-SCC-M0 and PDX-SCC-M11). In such clinical scenario, one might have to consider combination strategies with conventional chemotherapeutic drugs. Cisplatin typically causes regression of previously untreated HNSCC, and therefore it is the most frequently used chemotherapy in head and neck cancer. The problem is that advanced HNSCC treated with Cisplatin frequently end up recurring locally or at distant sites. We have previously shown that Cisplatin increases the CSC fraction by enhancing their self-renewal particularly in presence of IL-6 [10]. Considering that CSC cells appear to drive head and neck tumor recurrence [7,16,26], these results suggest the possible indication of combination therapy using an anti-IL-6 strategy and a conventional (de-bulking) chemotherapeutic drug.

We observed that low dose MEDI5117 (3 mg/kg) consistently decreased the fraction of CSC in all 3 PDX models of HNSCC tested

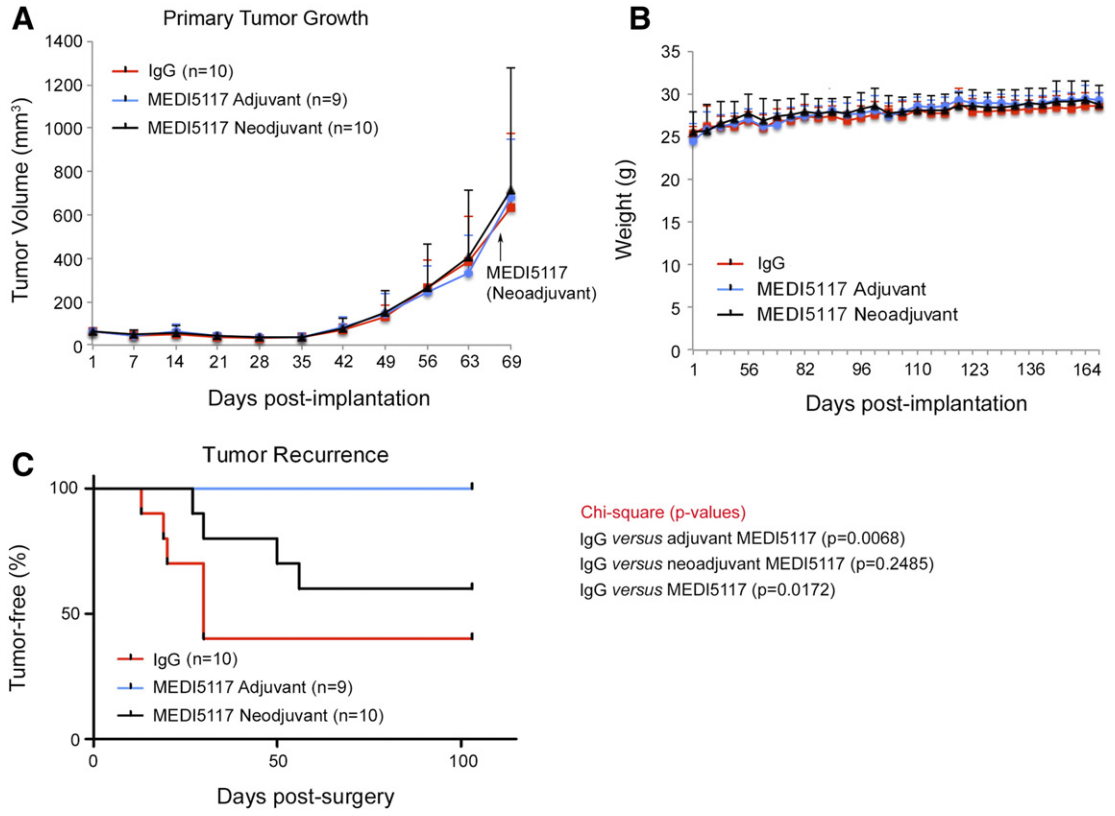

Figure 5. MEDI5117 prevents tumor recurrence when used in the adjuvant setting. (A) Graph depicting mean tumor growth (PDX-SCC-M0) over time in mice treated with MEDI5117, as compared to treatment with control IgG. Arrow denotes the timing for the beginning of treatment with MEDI5117 in the neoadjuvant setting. MEDI5117 was administered either in a *neoadjuvant* setting (treatment started 2 days prior to surgery) or *adjuvant* setting (treatment started 1 day after surgery). Mice from both groups were treated equally thereafter. The control IgG group received its first dose 1 day following surgical resection of the tumors, mimicking the adjuvant setting. Survival was defined as recurrence-free mice, as determined by the absence of a palpable secondary tumor mass measuring $\leq 100\ mm^3$. (B) Graph depicting average mouse weight according to treatment conditions over time. (C) Graph depicting the Kaplan-Meier analysis of the effect of MEDI5117 on tumor recurrence according to treatment regimen.

here. In contrast, high dose MEDI5117 (30 mg/kg) only reduced the fraction of cancer stem cells in the PDX-SCC-M11 model, which was generated from a patient that was previously treated with chemoradiation. These results are surprising, as one would perhaps expect that the results with higher concentration of MEDI5117 would be aligned with those with the low concentration. Nevertheless, when MEDI5117 was used in a PDX model generated from a previously untreated primary tumor, we observed a significant decrease in tumor growth rate, suggestive of an effect of MEDI5117 in both CSC as well as in more differentiated cells. This might explain why in this case we did not observe significant differences in the CSC fraction with 30 mg/kg MEDI5117, as the reduction in the number of CSC and non-CSC might have been proportionally similar. From these studies we concluded that a low dose MEDI5117 might be effective in reducing the fraction of CSC across diverse HNSCC tumors. As indicated above, possible combination strategies with a chemotherapeutic drug might benefit from the possibility of using low dose MEDI5117 as a means to reduce safety concerns while maintaining efficacy.

Perhaps the most intriguing aspect of this work is that the anti-IL-6 antibody eliminated tumor recurrence when used in the adjuvant setting immediately after surgical removal of the tumor. For these studies, we selected the PDX-SCC-M0 model generated from a recurrent human tumor as a way to challenge the anti-IL-6 therapy. Overall, MEDI5117 prevented tumor recurrence for 100 days post-surgery. When we break down the results by treatment regimen, we observed that the adjuvant treatment with MEDI5117 eliminated tumor recurrence, *i.e.* we had 0 recurrences by 100 days of follow-up in this group. Neoadjuvant dosing of MEDI5117 showed a trend (albeit non-significant) for reduction of tumor recurrence. In both cases, we did not observe significant toxicities despite the fact that the antibody was used for a long time, as demonstrated by the maintenance of mouse weight throughout the study. We postulate that the effect of MEDI5117 in preventing tumor recurrences might be correlated with its ability to inhibit the tumorigenic function of the cancer stem cells.

In conclusion, the work presented here represents the first attempt to determine the effect of the new monoclonal anti-IL-6 antibody MEDI5117 in head and neck squamous cell carcinoma. We are encouraged by the inhibitory effects of this antibody on the fraction of cancer stem cells and on the incidence of recurrence in PDX models that are representative of human disease. This work also unveiled important questions that will have to be answered with regard to the ideal dosing and regimen for maximal effect of this new putative therapy for HNSCC. While certainly much work still needs to be done to fully develop an anti-cancer stem cell therapy based on IL-6

inhibition, these results suggest that patients with head and neck cancer might benefit from therapeutic blockade of IL-6 signaling.

Acknowledgements

We thank the patients who kindly provided the tumor specimens used to generate the patient-derived xenograft (PDX) models needed for this research. We also thank the surgeons, nurses and support staff that enabled the process of tumor specimen collection and processing for use in research. We thank Zhaocheng Zhang for his assistance with immunohistochemistry; Thomas Carey for the UM-SCC-11B and UM-SCC-22B cell lines; and Rogerio Castillo for his assistance and expertise with fluorescence imaging. This work was funded through the MedImmune-University of Michigan Research Agreement.

Appendix A. Supplementary data

Supplementary data to this article can be found online at http://dx.doi.org/10.1016/j.neo.2016.03.004.

References

[1] Siegel R, Naishadham D, and Jemal A (2013). Cancer statistics, 2013. *CA Cancer J Clin* **63**(1), 11–30.

[2] Forastiere A, Koch W, Trotti A, and Sidransky D (2001). Head and neck cancer. *N Engl J Med* **345**(26), 1890–1900.

[3] Pulte D and Brenner H (2010). Changes in survival in head and neck cancers in the late 20th and early 21st century: a period analysis. *Oncologist* **15**(9), 994–1001.

[4] Reya T, Morrison SJ, Clarke MF, and Weissman IL (2001). Stem cells, cancer, and cancer stem cells. *Nature* **414**(6859), 105–111.

[5] Cho R and Clarke MF (2008). Recent advances in cancer stem cells. *Curr Opin Genet Dev* **18**, 48–53.

[6] Prince ME, Sivanandan R, Kaczorowski A, Wolf GT, Kaplan MJ, and Dalerba P, et al (2007). Identification of a subpopulation of cells with cancer stem cell properties in head and neck squamous cell carcinoma. *Proc Natl Acad Sci U S A* **104**(3), 973–978.

[7] Chinn SB, Darr OA, Owen JH, Bellile E, McHugh JB, Spector ME, Papagerakis SM, Chepeha DB, Bradford CR, and Carey TE, et al (2015). Cancer stem cells: mediators of tumorigenesis and metastasis in head and neck squamous cell carcinoma. *Head Neck* **37**(3), 317–326.

[8] Hermann PC, Bhaskar S, Cioffi M, and Heeschen C (2010). Cancer stem cells in solid tumors. *Semin Cancer Biol* **20**(2), 77–84.

[9] Diehn M, Cho RW, Lobo NA, Kalisky T, Dorie MJ, Kulp AN, Qian D, Lam JS, Ailles LE, and Wong M, et al (2009). Association of reactive oxygen species levels and radioresistance in cancer stem cells. *Nature* **458**(7239), 780–783.

[10] Nör C, Zhang Z, Warner KA, Bernardi L, Visioli F, Helman JI, Roesler R, and Nör JE (2014). Cisplatin induces Bmi-1 and enhances the stem cell fraction in head and neck cancer. *Neoplasia* **16**(2), 137–146.

[11] Krishnamurthy S and Nör JE (2012). Head and neck cancer stem cells. *J Dent Res* **91**(4), 334–340.

[12] Morrison SJ and Spradling AC (2008). Stem cells and niches: mechanisms that promote stem cell maintenance throughout life. *Cell* **132**(4), 598–611.

[13] Borovski T, De Sousa E, Melo F, Vermeulen L, and Medema JP (2011). Cancer stem cell niche: the place to be. *Cancer Res* **71**(3), 634–639.

[14] Krishnamurthy S, Dong Z, Vodopyanov D, Imai A, Helman JI, and Prince ME, et al (2010). Endothelial cell-initiated signaling promotes the survival and self-renewal of cancer stem cells. *Cancer Res* **70**(23), 9969–9978.

[15] Neiva KG, Zhang Z, Miyazawa M, Warner KA, Karl E, and Nör JE (2009). Cross talk initiated by endothelial cells enhances migration and inhibits anoikis of squamous cell carcinoma cells through STAT3/Akt/ERK signaling. *Neoplasia* **11**(6), 583–593.

[16] Zhang Z, Dong Z, Lauxen I, Sant'Anna M, and Nör JE (2014). Endothelial cell-secreted EGF induces epithelial to mesenchymal transition and endows head and neck cancer cells with stem-like phenotype. *Cancer Res* **74**(10), 2869–2881.

[17] Krishnamurthy S, Meyers K, Dong Z, Imai A, Ward B, Helman JI, Taichman R, Bellile EL, McCauley L, and Polverini PJ, et al (2014). Endothelial IL-6 defines the tumorigenic potential of human head and neck cancer stem-like cells. *Stem Cells* **32**(11), 2845–2857.

[18] Constantinescu SN, Girardot M, and Pecquet C (2008). Mining for JAK-STAT mutations in cancer. *Trends Biochem Sci* **33**(3), 122–131.

[19] Duffy SA, Taylor JM, Terrell JE, Islam M, Li Y, Fowler KE, Wolf GT, and Teknos TN (2008). Interleukin-6 predicts recurrence and survival among head and neck cancer patients. *Cancer* **113**(4), 750–757.

[20] Finch DK, Sleeman MA, Moisan J, Ferraro F, Botterell S, and Campbell J, et al (2011). Whole-molecule antibody engineering: generation of a high-affinity anti-IL-6 antibody with extended pharmacokinetics. *J Mol Biol* **411**(4), 791–807.

[21] Krishnamurthy S and Nör JE (2013). Orosphere assay: a method for propagation of head and neck cancer stem cells. *Head Neck* **35**(7), 1015–1021.

[22] Warner KA, Adams A, Bernardi L, Nör C, Finkel KA, and Zhang Z, et al (2013). Characterization of tumorigenic cell lines from the recurrence and lymph node metastasis of a human salivary mucoepidermoid carcinoma. *Oral Oncol* **49**(11), 1059–1066.

[23] Nims RW, Sykes G, Cottrill K, Ikonomi P, and Elmore E (2010). Short tandem repeat profiling: part of an overall strategy for reducing the frequency of cell misidentification. *In Vitro Cell Dev Biol Anim* **46**(10), 811–819.

[24] Kumar B, Cordell KG, Lee JS, Prince ME, Tran HH, and Wolf GT, et al (2007). Response to therapy and outcomes in oropharyngeal cancer are associated with biomarkers including human papillomavirus, epidermal growth factor receptor, gender, and smoking. *Int J Radiat Oncol Biol Phys* **69**(2 Suppl), S109–S111.

[25] Stransky N, Egloff AM, Tward AD, Kostic AD, Cibulskis K, and Sivachenko A, et al (2011). The mutational landscape of head and neck squamous cell carcinoma. *Science* **333**(6046), 1157–1160.

[26] Hildebrand LC, Carvalho AL, Lauxen IS, Nör JE, Cerski CT, and Sant'Ana Filho M (2014). Spatial distribution of cancer stem cells in head and neck squamous cell carcinomas. *J Oral Pathol Med* **43**(7), 499–506.